Nano Energy 24 (2016) 139–147

Contents lists available at ScienceDirect

Nano Energy

journal homepage: www.elsevier.com/locate/nanoen

Self-assembled ultrathin $NiCo_2S_4$ nanoflakes grown on Ni foam as high-performance flexible electrodes for hydrogen evolution reaction in alkaline solution

Lianbo Ma [a], Yi Hu [a], Renpeng Chen [a], Guoyin Zhu [a], Tao Chen [a], Hongling Lv [a], Yanrong Wang [a], Jia Liang [a], Haixia Liu [a], Changzeng Yan [a], Hongfei Zhu [a], Zuoxiu Tie [a], Zhong Jin [a,*], Jie Liu [a,b,**]

[a] Key Laboratory of Mesoscopic Chemistry of MOE and Collaborative Innovation Center of Chemistry for Life Sciences, School of Chemistry and Chemical Engineering, Nanjing University, Nanjing 210093, China
[b] Department of Chemistry, Duke University, Durham, NC 27708, USA

ARTICLE INFO

Article history:
Received 4 March 2016
Received in revised form
4 April 2016
Accepted 16 April 2016
Available online 19 April 2016

Keywords:
Hydrogen evolution reaction
Ultrathin $NiCo_2S_4$ nanoflakes
Layered double hydroxide
Three-dimensional-networked structure
Alkaline solution

ABSTRACT

Considerable efforts have been devoted on the design and fabrication of non-platinum electrocatalysts with high performance and low cost for hydrogen evolution reaction (HER). However, the catalytic activity of existing electrocatalysts usually subjects to the limited amount of exposed active sites. Herein, we propose that self-assembled ultrathin $NiCo_2S_4$ nanoflakes grown on nickel foam ($NiCo_2S_4$/Ni foam) can serve as excellent electrocatalyst for HER in alkaline solution with high activity and stability. The $NiCo_2S_4$/Ni foam electrodes were prepared by the complete sulfidation of networked ultrathin NiCo-layered double hydroxide nanoflakes grown on Ni foam (NiCo-LDH/Ni foam). The advantages of this unique architecture are that the ultrathin and porous $NiCo_2S_4$ nanoflakes can provide a huge number of exposed active sites, the highly-conductive Ni foam can promote the transfer of electrons, and the three-dimensional-networked structure can facilitate the diffusion and penetration of electrolyte. Electrochemical measurements reveal that $NiCo_2S_4$/Ni foam electrodes exhibit greatly improved performance than NiCo-LDH/Ni foam for HER in alkaline solution with low onset overpotential (17 mV), small Tafel slope (84.5 mV/dec) and excellent long-duration cycling stability (maintaining an onset overpotential of ~20 mV and an overpotential of 155 mV at 50 mA/cm^2 after testing for 100,000 s). In addition, the highly-flexible $NiCo_2S_4$/Ni foam electrodes show no obvious catalytic degradation after bending for 200 times, confirming the high flexibility and robustness under severe conditions.

1. Introduction

Hydrogen has been considered as a clean resource to replace the diminishing fossil fuels due to its ultrahigh gravimetric energy density among existing fuels [1,2]. The reforming of nature gas or methane is a conventional approach of hydrogen generation for industrial purposes [3,4], but the problem of CO_2 release during this process seriously restricts its extensive application [5]. In recent years, hydrogen generation from water splitting has presented an alternative eco-friendly and carbon-free strategy for hydrogen production [6], but a necessity for carrying out the hydrogen evolution reaction (HER, In acidic solution: $2H^+ + 2e^- \rightarrow H_2$; In alkaline solution: $2H_2O + 2e^- \rightarrow H_2 + 2OH^-$) is the use of electrocatalysts [7–9]. Platinum (Pt) and other Pt-group metals have been considered as the best catalysts for HER [10]. Unfortunately, the low natural abundance and high cost of Pt-group noble metals restrict their massive deployment for hydrogen production. Therefore, the design and fabrication of novel electrocatalysts for HER with minimum noble metal usage is in urgent demand.

To realize this goal, various electrocatalysts have been developed. Until now, metal alloys [11,12], transition metal chalcogenides [13,14], nitrides [15,16], carbides [17,18], and phosphides [19,20] are the most widely investigated catalysts for replacing Pt-group metals because of their high stability, high abundance and low cost. However, these catalysts usually suffer from lower electrical conductivity

* Corresponding author.
** Corresponding author at: Key Laboratory of Mesoscopic Chemistry of MOE and Collaborative Innovation Center of Chemistry for Life Sciences, School of Chemistry and Chemical Engineering, Nanjing University, Nanjing 210093, China.
E-mail addresses: zhongjin@nju.edu.cn (Z. Jin), j.liu@duke.edu (J. Liu).

http://dx.doi.org/10.1016/j.nanoen.2016.04.024
2211-2855/

and/or limited number of exposed active sites, which seriously limit their catalytic performance toward HER [21]. Recently, it was acknowledged that two effective strategies to improve the HER performance of electrocatalysts are: (1) the incorporation of catalytic materials with conductive networks; (2) the construction of special structures, such as hollow, porous, or hierarchical architectures [22–25]. Benefiting from their structural advantages, rationally-designed electrocatalysts may exhibit enhanced catalytic activity and stability (Table S1) [5,23,24,26–44].

As we know, normally much larger overpotentials are needed to trigger the HER process in alkaline solution as compared with those in neutral and acidic solutions [8,24,27], and the exploration of novel electrocatalysts with high catalytic activity in alkaline solution remains a great challenge. With the merits of high surface-to-volume ratio, short diffusion length for carrier transport, composition versatility, easily-tailored properties and low cost, transition-metal layered double hydroxides (LDHs) have emerged as a novel class of electrocatalysts in alkaline solution [26,45,46]. Interestingly, we have noticed that LDHs also can serve as versatile precursors to produce a variety of other multicomponent transition-metal compounds that may exhibit even better electrocatalytic performance than LDHs for HER in alkaline solution. Recently, it has been confirmed that the coordination structure of transition-metal dichalcogenides is similar to the active centers in hydrogenase [47], and the charged states of metals and sulfur in metal sulfides are similar to those of hydride-acceptors and proton-acceptors in hydrogenase and its analogues [35,48]. In addition, it is expected that the different electrocatalytic components would exhibit beneficial synergistic effect. Inspired by these, we then decide to take advantage of the unique structure of multi-metallic LDHs in the design of new electrocatalysts with further improved HER activity and stability. Herein, we demonstrate that three-dimensional-networked (3D-networked) NiCo-layered double hydroxide nanoflakes grown on Ni foam (NiCo-LDH/Ni foam) can be converted to ultrathin and porous $NiCo_2S_4$ nanoflakes on Ni foam ($NiCo_2S_4$/Ni foam) by a sulfidation process. Electrochemical measurements revealed that the binder-free, self-supported and highly-flexible $NiCo_2S_4$/Ni foam electrode exhibited much better electrocatalytic activity than NiCo-LDH/Ni foam in alkaline solution with low onset overpotential, small Tafel slope, and excellent catalytic retention during long-term tests (100,000 s) (Table S1). Remarkably, the mechanically flexible and robust characteristics of Ni foam ensure the widely application of $NiCo_2S_4$/Ni foam electrodes for HER under harsh circumstances.

2. Experimental

2.1. Chemicals

All the chemicals were purchased from Sinopharm Chemical Reagent Corp. with analytical grade and were used without further purification.

2.2. Synthesis of NiCo-LDH/Ni foam

Ni foams were cleaned in 1.0 M HCl solution with sonication for 10 min to remove nickel oxide on the surface, and subsequently washed with excessive deionized water and ethanol. In a typical synthesis, 290 mg of $Co(NO_3)_2 \cdot 6H_2O$, 145 mg of $Ni(NO_3)_2 \cdot 6H_2O$ and 600 mg of hexamethylenetetramine (HMT) were dissolved into 30 mL of methanol solution under stirring to form a clear solution. Then a piece of Ni foam (2 cm × 1 cm) was put into the solution, and transferred into a Teflon-lined stainless steel autoclave. After heating at 180 °C for about 12 h, the Ni foam was taken out and cleaned by sonication in deionized water for 2 min to remove any possible contamination on the surface.

2.3. Synthesis of $NiCo_2S_4$/Ni foam

Typically, the as-obtained NiCo-LDH/Ni foam was added into 30 mL of aqueous solution containing 300 mg of thioacetamide, and then the mixture was transferred into an autoclave and heated at 140 °C for 5 h. After cooling down to room temperature naturally, the product was washed with deionized water and ethanol for three times, respectively, and dried at 60 °C overnight.

2.4. Characterizations

The morphology, size and structure of the products were examined by field-emission scanning electron microscopy (FESEM, JSM-6480), transmission electron microscopy (TEM, JEM-2100) and Energy-dispersive X-ray spectroscope (EDX) attached to the FESEM. The crystallinity of as-synthesized samples were characterized by powder X-ray diffraction (XRD) on a Bruker D-8 Advance diffractometer using Cu Kα ($\lambda = 1.5406$ Å) radiation at a scanning rate of 6°/min. X-ray photoelectron spectra (XPS) were obtained using a PHI-5000 VersaProbe X-ray photoelectron spectrometer with an Al Kα X-ray radiation. Raman spectra were collected with a Horiba JY H800 Raman spectrometer using a 532 nm laser source.

2.5. Electrochemical measurements

The catalytic performances of the as-prepared samples toward HER were conducted on a typical three-electrode setup using a CHI 760D electrochemical analyzer (Chenhua Instruments, Shanghai) at room temperature. Ni foam, NiCo-LDH/Ni foam or $NiCo_2S_4$/Ni foam were separately used as the working electrodes. Saturated calomel electrode (SCE) and Pt foil were used as the reference and counter electrodes, respectively. Cyclic voltammetry (CV), electrochemical impedance spectroscopy (EIS), chronoamperometry measurements and chronopotentiometric measurements were conducted, and linear sweep voltammetry (LSV) was performed at a scan rate of 2 mV/s. During the electrochemical measurements, the electrolyte (1.0 M KOH, pH = 14.0) was degassed by bubbling high-purity nitrogen to eliminate the dissolved oxygen. During the HER stability tests, the pH value usually only slightly change from 14.0 to approximately 14.2 after HER testing for 6 h, this tiny increment of pH value has very little influence on the electrochemical results. In addition, to eliminate the influence of the pH variation, a pH detector was employed to monitor the pH value of electrolyte, and a certain amount (~5 mL) of deionized water was added into the reaction system with a time interval of 6 h to maintain a relatively stable pH value of 14.0 in the reaction system. The calculation of current densities was based on the actual area of electrode that immersed in the electrolyte, and the height of electrode was carefully adjusted according to the height of electrolyte level. All the potentials measured in our work were calibrated with the reversible hydrogen electrode (RHE) according to the equation: $E_{RHE} = E_{SCE} + 0.2412 + 0.05916 \times pH$.

3. Results and discussion

As schematically illustrated in Fig. 1a, the 3D-networked $NiCo_2S_4$/Ni foam electrode was fabricated *via* a two-step strategy. In the first hydrothermal synthesis step, Ni foam was immersed into an aqueous solution containing Ni^{2+} and Co^{2+}. The OH^- ions gradually released by the hydrolysis of hexamethylenetetramine (HMT) at high temperature facilitated the formation and uniform assembly of NiCo-layered double hydroxide (NiCo-LDH) nanoflakes on the entire surface of the Ni foam. In the second sulfurization process, the as-prepared NiCo-LDH nanoflakes on Ni foam were converted to ultrathin and porous $NiCo_2S_4$ nanoflakes with well-retained morphology. The

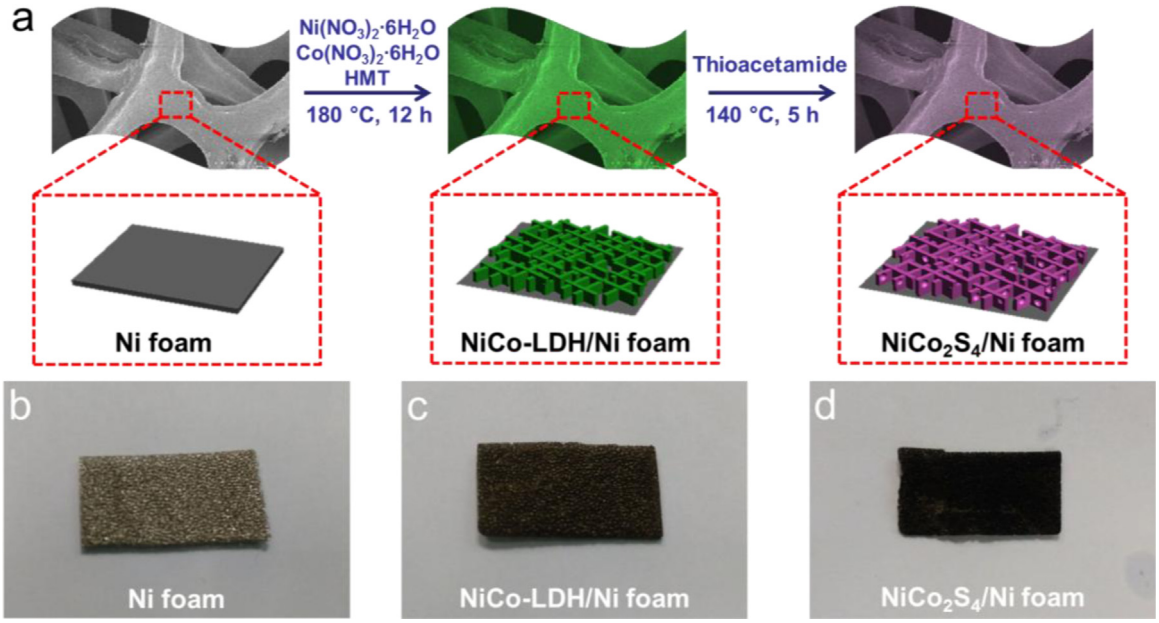

Fig. 1. (a) Schematic illustration of the two-step strategy for preparing 3D-networked NiCo-LDH/Ni foam and $NiCo_2S_4$/Ni foam electrodes. Optical images of (b) initial Ni foam, (c) as-prepared NiCo-LDH/Ni foam and (d) $NiCo_2S_4$/Ni foam, respectively.

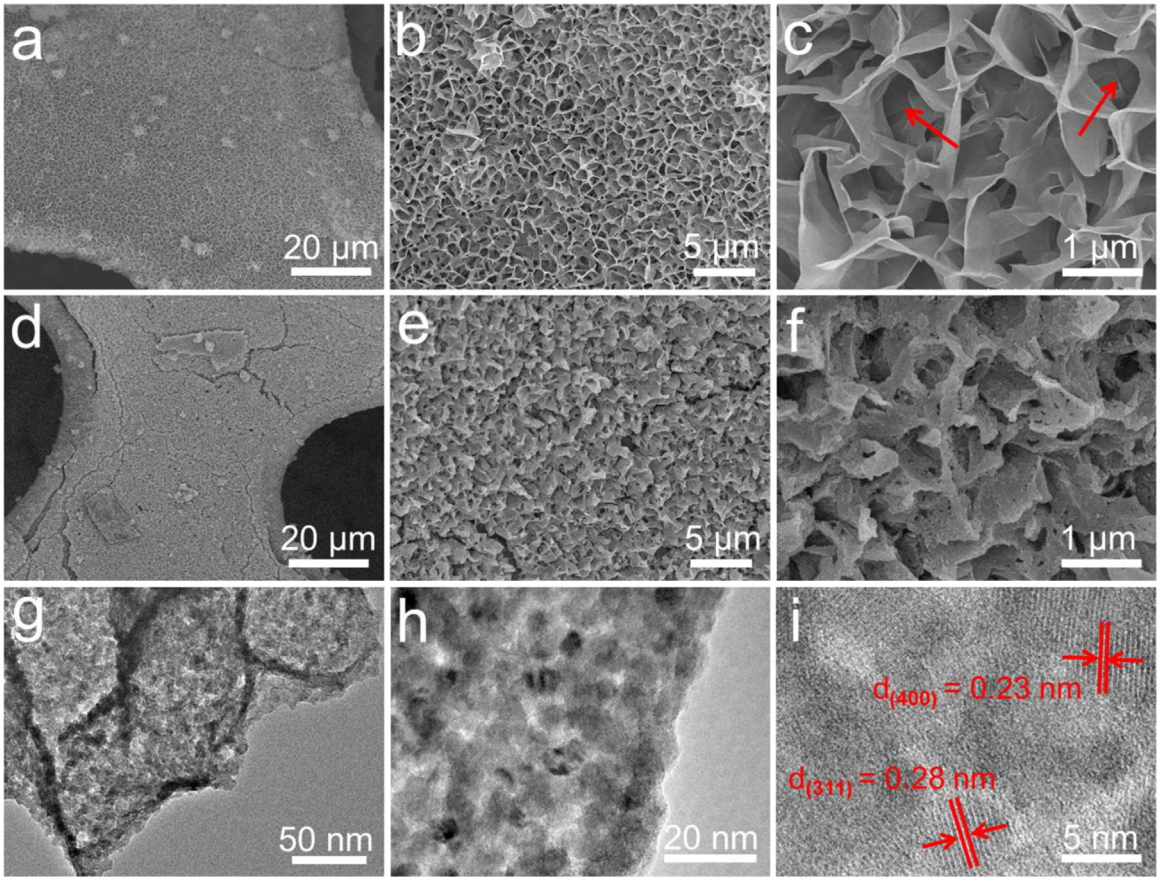

Fig. 2. (a-c) FESEM images of the NiCo-LDH/Ni foam, revealing that the ultrathin NiCo-LDH nanoflakes interconnected and intersected with each other to form a networked structure. The red arrows in (c) indicate the void spaces between the NiCo-LDH nanoflakes. (d-f) FESEM images and (g-i) TEM images of the 3D-networked $NiCo_2S_4$/Ni foam architecture. The morphology of $NiCo_2S_4$/Ni foam is similar to that of NiCo-LDH/Ni foam, but with numerous pores formed in the nanoflakes. (i) The HRTEM image of $NiCo_2S_4$/Ni foam indicates two lattice distances of 0.23 and 0.28 nm, corresponding to the (400) and (311) planes of $NiCo_2S_4$, respectively.

optical images of initial Ni foam and the as-prepared products after two sequential steps are also provided in Fig. 1b-d, which suggest the high structural integrity and the color changes of the products with 3D-networked architectures.

Field-emission scanning electron microscopy (FESEM) and transmission electron microscopy (TEM) were applied to examine the morphology and microstructure of the products. The typical FESEM image of bare Ni foam is presented in Fig. S1, which shows

networked structure and clean surface. Fig. 2a-c present the FESEM images of NiCo-LDH/Ni foam. It could be seen that the surface of Ni foam was evenly covered by NiCo-LDH nanoflakes (Fig. 2a), and no exposed surface of Ni foam was observed. FESEM images with higher magnification (Fig. 2b and c) revealed that densely-packed, highly-ordered NiCo-LDH nanoflakes were grown on Ni foam surface. The NiCo-LDH nanoflakes were interconnected and intersected with each other to form a 3D-networked structure with plenty of void spaces (marked by red arrows in Fig. 2c). Further TEM characterization (Fig. S2) reveals that the thickness of NiCo-LDH sheets is in the range of 3–5 nm. After the sulfurization process, the interconnected and intersected structure was well retained, as shown in the FESEM images of $NiCo_2S_4$/Ni foam (Fig. 2d-f). Numerous pores were formed in the $NiCo_2S_4$ nanoflakes, which may be attributed to the formation of H_2S released from the decomposition of thioacetamide during the sulfurization step. Fig. 2g-i presents the TEM images of the $NiCo_2S_4$/Ni foam architecture. Wrinkled nanoflakes composed of agglomerative $NiCo_2S_4$ nanoparticles were observed (Fig. 2g), and the fine particles of $NiCo_2S_4$ showed a size range of 10–15 nm (Fig. 2h). The high-resolution TEM (HRTEM) image (Fig. 2i) reveals two distinct lattice spacings of 0.23 and 0.28 nm corresponding to the (400) and (311) planes of $NiCo_2S_4$, respectively, confirming the formation of $NiCo_2S_4$ nanocrystals. The 3D-networked and porous $NiCo_2S_4$/Ni foam is reckoned to be very beneficial for electrocatalysis process because: (i) the ultrathin and porous $NiCo_2S_4$ nanoflakes provide a great number of exposed active sites for expediting the HER process, (ii) the abundant pores and void spaces between nanoflakes facilitate the diffusion and penetration of ions and electrons during the electrochemical reactions [49], and (iii) the Ni foam provides strong mechanical strength and excellent electrical conductivity for the transport of electrons [50].

The as-prepared NiCo-LDH/Ni foam and $NiCo_2S_4$/Ni foam products were comprehensively characterized by X-ray diffraction (XRD), energy dispersive X-ray spectroscopy (EDX), Raman spectroscopy and X-ray photoelectron spectroscopy (XPS). The XRD characterization (Fig. S3) of NiCo-LDH/Ni foam indicates the successful preparation of NiCo-LDH (JCPDS card No. 33-0429, space group: $R^{**}(166)$, $a=3.038$, $b=3.038$, $c=22.790$). Fig. 3a shows the XRD pattern of 3D-networked ultrathin $NiCo_2S_4$/Ni foam product, except the strong diffraction peaks of Ni foam, all other diffraction peaks can be accordingly indexed to the cubic phase $NiCo_2S_4$ (JCPDS card No. 20–0782, space group: $Fd\text{-}3m(227)$, $a=9.387$, $b=9.387$, $c=9.387$), confirming the formation of $NiCo_2S_4$ in the sulfurization process. The EDX spectrum of NiCo-LDH/Ni foam (Fig. S4) demonstrates the co-existence of Ni, Co, and O elements; while in the EDX spectrum of $NiCo_2S_4$/Ni foam (Fig. S5), the O element almost disappeared and the S element was detected instead. Moreover, further Raman characterizations (Figs. S6 and S7) confirmed the preparation of NiCo-LDH and $NiCo_2S_4$, respectively. The survey XPS spectrum of $NiCo_2S_4$/Ni foam (Fig. S8) is consistent with the above result of EDX. In the high-resolution XPS spectrum of Ni 2p region (Fig. 3b), two spin-orbit doublets can be deconvoluted by using the Gaussian fitting method, which are attributed to the characteristics of Ni^{2+} and Ni^{3+}, and two shake-up satellite peaks, respectively. The intense satellite peaks indicate that the majority of Ni element in the final product is Ni^{2+} cations [51], which is in good agreement with that of $NiCo_2S_4$. As regards the Co

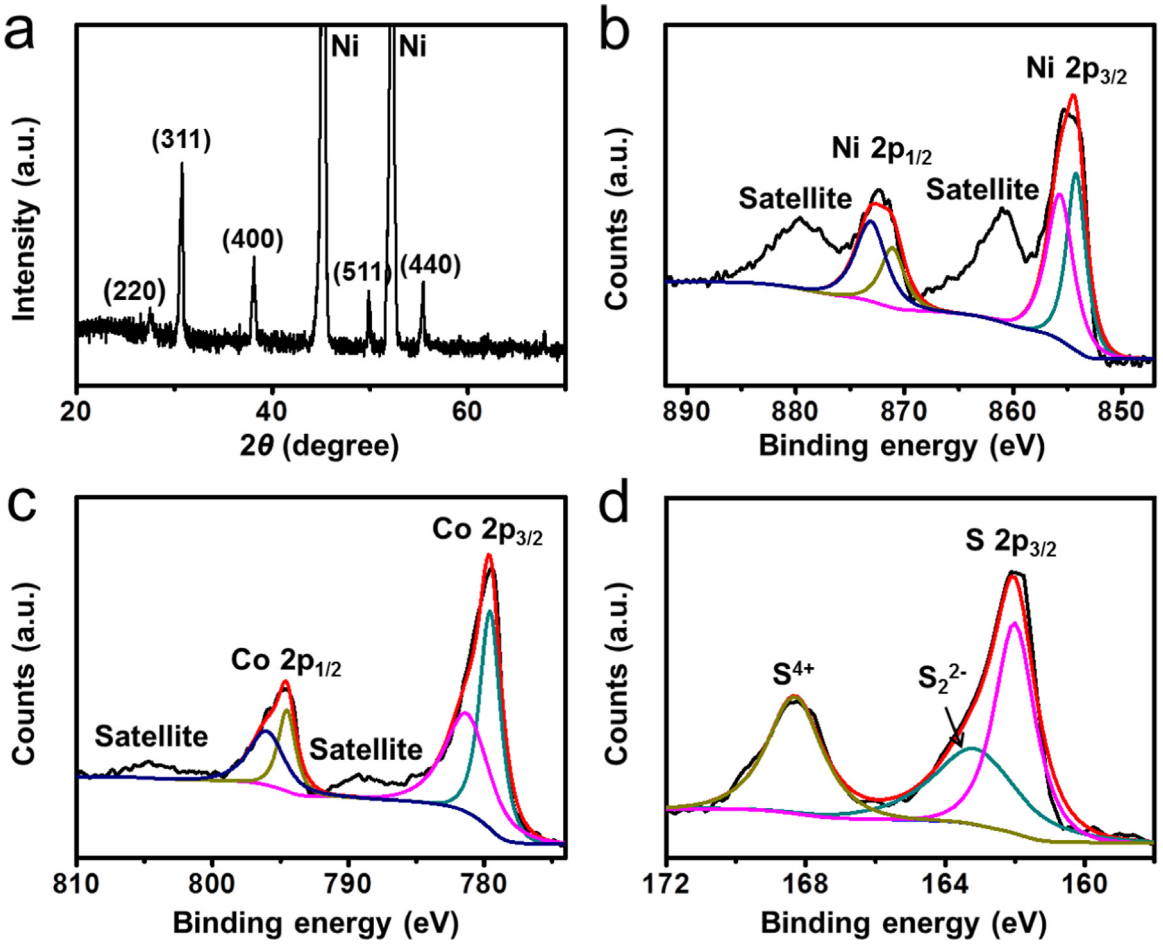

Fig. 3. (a) XRD pattern, high-resolution XPS spectrum of (b) Ni 2p region, (c) Co 2p region, and (d) S 2p region of the 3D-networked ultrathin $NiCo_2S_4$/Ni foam architecture.

2p region (Fig. 3c), it shows two distinguished doublets located at a low energy band (Co $2p_{3/2}$) and a high energy band (Co $2p_{1/2}$), respectively. The difference of binding energy between the two doublets is over 15 eV, suggesting the co-existence of Co^{2+} and Co^{3+} [52]. Fig. 3d shows the core-level spectrum of S 2p region, and the binding energy of 161.8 eV is corresponding to S $2p_{3/2}$. In detail, the deconvoluted peak at 163.6 eV is originated from the sulfur-metal bonds, while the binding energy at 161.8 eV is attributed to the S^{2-} in low coordination at the surface [49,53,54]. The high energy of 168.7 eV is attributed to the S^{4+} species at the surface and/or edges of $NiCo_2S_4$ nanoflakes with highly oxidized state [53].

The samples with unique compositions and 3D-networked structure were then investigated as free-standing electrodes for electrocatalytic HER in 1.0 M KOH electrolyte. The linear sweep voltammetry (LSV) measurements were performed to estimate the HER activity of $NiCo_2S_4$/Ni foam, and control experiments on NiCo-LDH/Ni foam and bare Ni foam were also conducted for comparison. As shown in Fig. 4a, the LSV polarization curve of $NiCo_2S_4$/Ni foam exhibit an onset overpotential of only 17 mV, which is much smaller than those of NiCo-LDH/Ni foam (67 mV) and bare Ni foam (150 mV). This result suggests that the surface of $NiCo_2S_4$/Ni foam is much more active for HER. The overpotential at the cathodic current density of 10 mA/cm^2 (η_{10}) can be used to evaluate the HER activity

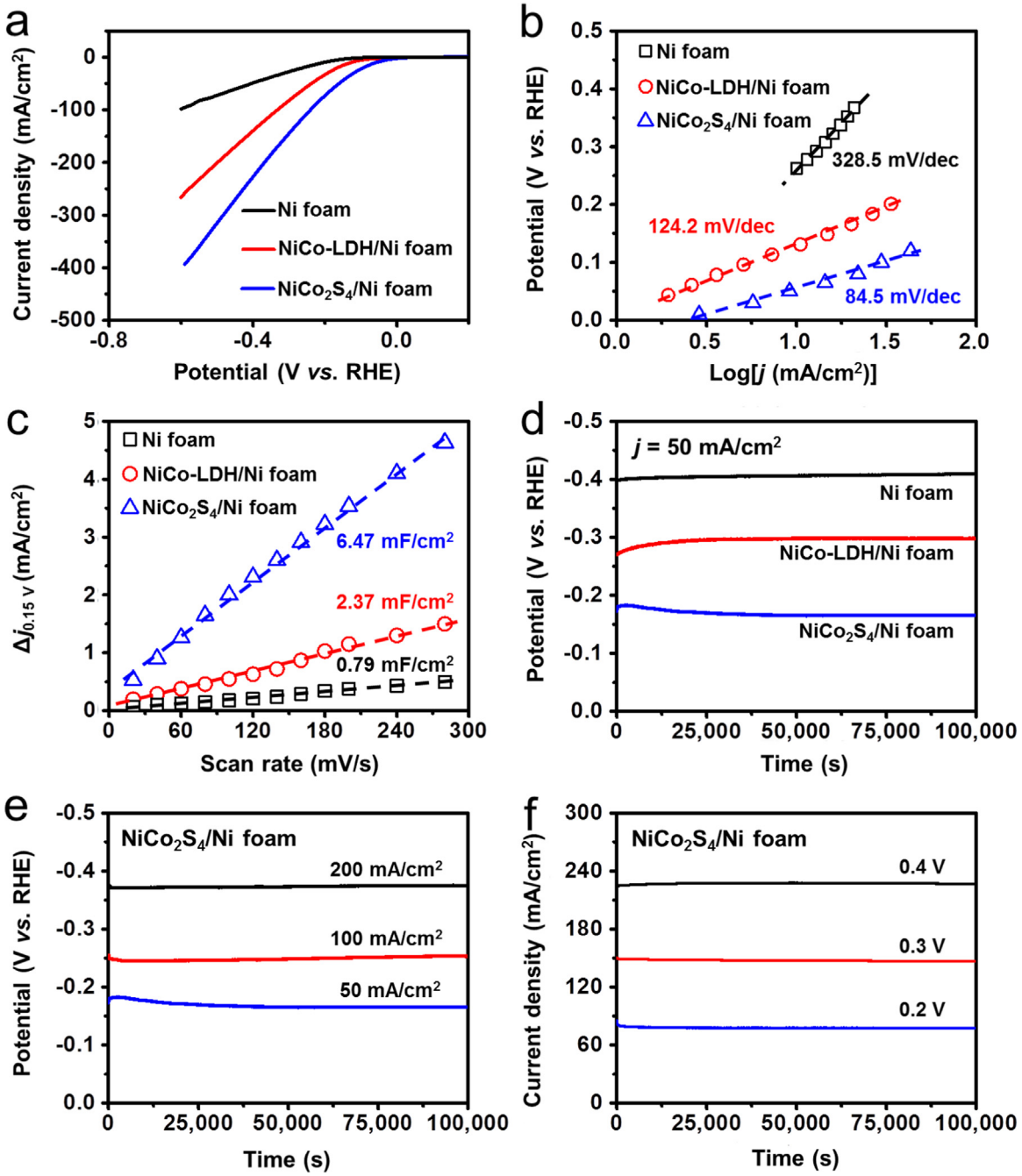

Fig. 4. (a) LSV polarization curves and (b) the corresponding Tafel slopes of bare Ni foam, NiCo-LDH/Ni foam and $NiCo_2S_4$/Ni foam electrodes. (c) The capacitive currents at 0.15 V as a function of scan rate for bare Ni foam, NiCo-LDH/Ni foam and $NiCo_2S_4$/Ni foam. (d) Chronopotentiometric measurements of long-term stability of bare Ni foam, NiCo-LDH/Ni foam and $NiCo_2S_4$/Ni foam at a current density of 50 mA/cm^2. (e) Chronopotentiometric measurements of long-term stability of $NiCo_2S_4$/Ni foam electrodes at various current densities (50, 100 and 200 mA/cm^2). (f) Chronoamperometry curves of long-term stability of $NiCo_2S_4$/Ni foam electrodes under various overpotentials (0.2, 0.3 and 0.4 V).

of electrocatalysts [55]. The η_{10} of $NiCo_2S_4$/Ni foam was approaching 65 mV, significantly lower than those of NiCo-LDH/Ni foam (140 mV) and bare Ni foam (240 mV). Based on the LSV polarization curves in Fig. 4a, corresponding Tafel plots were calculated (Fig. 4b). The Tafel plots of these catalysts fitted very well with the Tafel equation ($\eta = b \times \log j + a$, where j is the current density and b is the Tafel slope) at different overpotential ranges. The Tafel slopes of $NiCo_2S_4$/Ni foam, NiCo-LDH/Ni foam and bare Ni foam were *ca.* 84.5, 124.2 and 328.5 mV/dec, respectively. It proves that the 3D-networked $NiCo_2S_4$/Ni foam electrode exhibits the highest catalytic activity toward HER among all these samples. According to the previous reports [56–58], the mechanism of HER process in alkaline solution can be regarded as a combination of three basic steps: (1) the electroreduction of water molecules and hydrogen adsorption (Volmer reaction: $M + H_2O + e^- \rightarrow M\text{–}H_{ads} + OH^-$), (2) the electrochemical hydrogen desorption (Heyrovsky reaction: $M\text{–}H_{ads} + H_2O + e^- \rightarrow M + H_2 + OH^-$), and/or (3) the chemical desorption (Tafel reaction: $2M\text{–}H_{ads} \rightarrow 2M + H_2$), where M stands for an metal atom, and H_{ads} represents a H atom absorbed at an active site of the catalyst. The relative low Tafel slope indicates that the HER process with $NiCo_2S_4$/Ni foam as the electrocatalyst in alkaline solution is more facile. Moreover, compared to the previously-reported electrocatalysts for HER in alkaline solution (Table S1) [5,23,24,26–44], the $NiCo_2S_4$/Ni foam electrode in this work shows remarkable electrocatalytic activity.

It is known that the HER catalytic activity of electrocatalysts depends largely on the electrochemically-active surface area (ECSA) [59,60]. To estimate the effective ECSA of these samples, we measured the electric double layer capacitance (EDLC) at the solid/liquid interface of all electrodes. The CV curves were collected in the region of 0.1–0.2 V, where the current responses should only be due to the charging/discharging of electrical double layers on the surface of electrodes (Fig. S9). Fig. 4(c) shows the capacitive currents at 0.15 V as a function of scan rate for all samples, the EDLCs of $NiCo_2S_4$/Ni foam, NiCo-LDH/Ni foam and bare Ni foam were *ca.* 6.47, 2.37, and 0.79 mF/cm^2, respectively, showing that $NiCo_2S_4$/Ni foam has a much higher effective ECSA than other samples. It indicates that the much better HER catalytic activity of $NiCo_2S_4$/Ni foam may be associated with its higher effective surface area and larger amount of active sites.

The estimation of turnover frequency (TOF) for each active sites makes it possible to compare the catalytic activity of $NiCo_2S_4$/Ni foam with other reported HER catalysts. The number of the active sites was quantified following the previous literature [35,61]. Fig. S10 shows the cyclic voltammetry (CV) curve at 50 mV s^{-1} in phosphate buffered saline (PBS, pH = 7.0) solution. Assuming a one-electron process occurred for both reduction and oxidation, the upper limit of active sites could be calculated. Fig. S11 displays the polarization curve at pH = 14.0, normalized by the active sites and expressed in terms of TOF. As the most active catalyst, Pt shows a TOF of 0.8 s^{-1} at the overpotential of 0 mV [13], while $NiCo_2S_4$/Ni foam needs an overpotential of 35 mV. To achieve the TOF values of 4.0 and 7.0 s^{-1}, $NiCo_2S_4$/Ni foam needs overpotentials of 110 and 155 mV, respectively. The as-obtained TOF values are higher than those of other reported HER catalysts under the same overpotentials [35,62–65], further suggesting the remarkable HER catalytic activity of $NiCo_2S_4$/Ni foam.

We also applied electrochemical impedance spectroscopy (EIS) measurements to further verify the conductivity advantages of $NiCo_2S_4$/Ni foam. As shown in Fig. S12, bare Ni foam exhibits the best ionic and Ohmic resistances due to its highly-conductive nature, and the $NiCo_2S_4$/Ni foam electrode displays much better impedance characteristics as compared with NiCo-LDH/Ni foam. The greatly enhanced ionic conductance and electronic conductivity of $NiCo_2S_4$/Ni foam electrode can be partly attributed to its unique compositions of bimetallic sulfide, of which the conductivity is much higher than transition-metal LDHs.

To evaluate the electrochemical stability of these electrodes, chronopotentiometric measurements of HER based on $NiCo_2S_4$/Ni foam, NiCo-LDH/Ni foam and bare Ni foam samples were carried out at a constant current density of 50 mA/cm^2, as shown in Fig. 4d. Remarkably, the $NiCo_2S_4$/Ni foam exhibited a overpotential slightly decreased from 178 mV to 165 mV after an long testing time of 100,000 s, indicating its increased catalytic activity toward HER. In contrast, under the same conditions, the NiCo-LDH/Ni foam showed an overpotential slightly increased to 300 mV, and the overpotential of bare Ni foam remained almost unchanged at a high value (400 mV). The galvanostatic measurements of $NiCo_2S_4$/Ni foam were also carried out at 100 and 200 mA/cm^2, respectively, as shown in Fig. 4e. It shows that the overpotential of $NiCo_2S_4$/Ni foam during long-term tests at each current density remained almost stable, demonstrating an ultra-high electrochemical stability compared to other existing electrocatalysts (Table S1) [5,23,24,26–44]. The long-duration chronoamperometric studies of $NiCo_2S_4$/Ni foam at 0.2, 0.3, and 0.4 V were performed, as shown in Fig. 4f. No obvious decrease in current density during long-term tests under different overpotential values was observed, further suggesting the excellent stability of $NiCo_2S_4$/Ni foam. The surface morphology and microstructure of the $NiCo_2S_4$/Ni foam electrode was retained very well after long-duration test for 100,000 s (Fig. S13), which confirms its high structural stability.

According to the above results, the $NiCo_2S_4$/Ni foam exhibits much higher electrocatalytic performance than NiCo-LDH/Ni foam, which may be attributed to the special compositions and unique nanostructure of $NiCo_2S_4$: (1) the first-row transition-metal dichalcogenides possess coordination structure similar to the active centers in effective hydrogenase [47], and the charged natures of metals and sulfur in metal sulfides are similar to those of hydride-acceptors and proton-acceptors in hydrogenase and its analogues [35,48]. (2) $NiCo_2S_4$ has much better electrical conductivity than NiCo-LDH (according to the EIS measurements in Fig. S12), which can promote the transfer of electrons, and thus boosting the HER process. (3) The hierarchical and porous characteristics of $NiCo_2S_4$ nanoflakes (as compared in Fig. 2c and f) can facilitate the penetration and migration of electrolyte, provide shorten pathways for electrons transfer, and exhibit much more exposed active sites for HER.

To further identify its high flexibility and structural integrity inherited from bare Ni foam [66,67], we investigated the HER performance of $NiCo_2S_4$/Ni foam electrode after bending for different times (Fig. 5a-d). As shown in Fig. 5e, the electrochemical activity of $NiCo_2S_4$/Ni foam electrode remained almost unchanged at the initial state (without bending) or after bending for 50, 100 and 200 times. The long stability test of $NiCo_2S_4$/Ni foam electrode after bending for 200 times was conducted at a constant current density of 50 mA/cm^2 (Fig. 5f). Compared with the stability tests in Fig. 4d, the $NiCo_2S_4$/Ni foam after bending for 200 times shows comparable long time cycling stability. In Fig. 4d, the $NiCo_2S_4$/Ni foam exhibited an overpotential decreased slightly from 178 mV to 165 mV after a long testing time of 100,000 s at a constant current density of 50 mA/cm^2. However, when the $NiCo_2S_4$/Ni foam was tested as electrocatalysts for HER after bending for 200 times, it has already been fully activated in the electrolyte owing to the previous LSV tests at initial state and after bending for 50, 100 and 200 times (Fig. 5e), therefore, the initial overpotential values in Figs. 4d and 5f are slightly different. During the long time stability tests after bending for 200 times, the overpotential of $NiCo_2S_4$/Ni foam increases from an initial value of 156 mV to 166 mV eventually. This corresponds to a potential increase of only 6.4% after a long period time (100,000 s), suggesting the excellent electrocatalytic stability of $NiCo_2S_4$/Ni foam and the great robustness

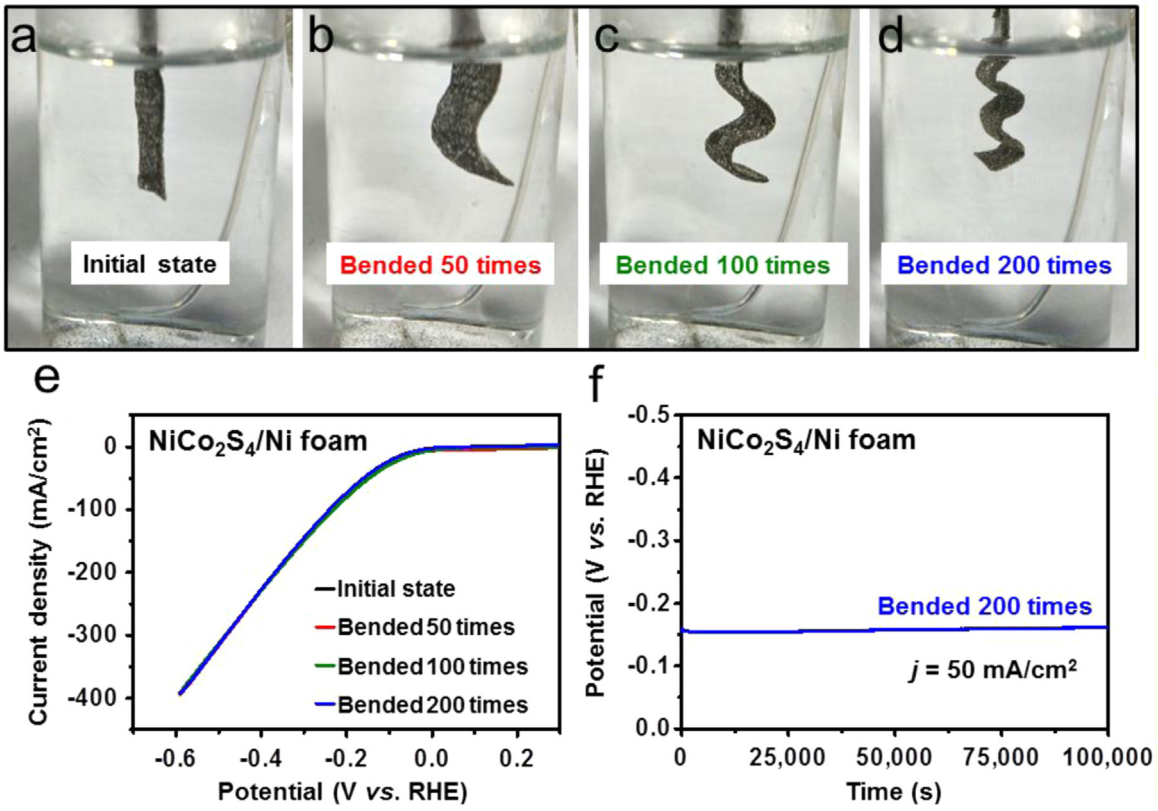

Fig. 5. Photographs of $NiCo_2S_4$/Ni foam electrodes during testing at (a) initial state (without bending) and after bending for (b) 50, (c) 100 and (d) 200 times, respectively. (e) The LSV polarization curves of $NiCo_2S_4$/Ni foam electrode at initial state and after bending for different times. (f) Long-term chronopotentiometric measurements of $NiCo_2S_4$/Ni foam electrode at a current density of 50 mA/cm^2 after bending for 200 times.

against external intervention. The high flexibility and structural durability of electrode are expected to be very beneficial to various applications, such as flexible photoelectrodes for photoelectrocatalysis, flexible fuel cells, portable hydrogen fuel device and so on.

4. Conclusions

In summary, we have rationally designed and fabricated 3D-networked $NiCo_2S_4$/Ni foam electrode as a high-performance HER electrocatalyst through the sulfidation of NiCo-LDH/Ni foam. Electrochemical measurements prove that the ultrathin and porous $NiCo_2S_4$/Ni nanoflakes on Ni foam can provide a high number of exposed active sites and facilitate the transport of electrons and ions. Therefore, the $NiCo_2S_4$/Ni foam electrode exhibits greatly enhanced catalytic performance in alkaline solution as compared with NiCo-LDH/Ni foam. Moreover, flexible $NiCo_2S_4$/Ni foam electrode shows almost no catalytic degradation after long-duration testing or after bending for many times. The high activity and stability make $NiCo_2S_4$/Ni foam a promising electrocatalyst, and the fabrication strategy can be extended to prepare other hierarchical and multicomponent compound electrodes for diverse electrochemical applications.

Acknowledgements

This work was supported by the National Thousand Young Talents Program of China, the Young Scientists Project of National Basic Research Program of China (973 Program No. 2015CB659300), the National Natural Science Foundation of China (NSFC Grant Nos. 21403105; 21573108), National Science Foundation for Post-doctoral Scientists of China (Grant Nos. 2015M581769, 2015M580413, and 2015M580408), the Jiangsu Province Science Foundation for Youths (Project No. BK20150571; BK20150583), the Fundamental Research Funds for the Central Universities and a project funded by the Priority Academic Program Development of Jiangsu Higher Education Institutions (PAPD).

Appendix A. Supplementary material

Supplementary data associated with this article can be found in the online version at http://dx.doi.org/10.1016/j.nanoen.2016.04.024.

References

[1] J.A. Turner, Science 305 (2004) 972–974.
[2] S. Han, Y.L. Feng, F. Zhang, C.Q. Yang, Z.Q. Yao, W.X. Zhao, F. Qiu, L.Y. Yang, Y. F. Yao, X.D. Zhuang, X.L. Feng, Adv. Funct. Mater. 25 (2015) 3899–3906.
[3] M.A. Rosen, D.S. Scott, Int. J. Hydrog. Energy 23 (1998) 653–659.
[4] D. Trommer, F. Noembrini, A. Fasciana, D. Rodriguez, A. Morales, M. Romero, A. Steinfeid, Int. J. Hydrog. Energy 30 (2005) 605–618.
[5] T.W. Lin, C.J. Liu, C.S. Dai, Appl. Catal. B 154 (2014) 213–220.
[6] T.R. Cook, D.K. Dogutan, S.Y. Reece, Y. Surendranath, T.S. Teets, D.G. Nocera, Chem. Rev. 110 (2010) 6474–6502.
[7] M. Dresselhaus, I. Thomas, Nature 414 (2001) 332–337.
[8] A.J. Bard, M.A. Fox, Acc. Chem. Res. 28 (1995) 141–145.
[9] M.G. Walter, E.L. Warren, J.R. McKone, S.W. Boettcher, Q. Mi, E.A. Santori, N. S. Lewis, Chem. Rev. 110 (2010) 6446–6473.
[10] D. Merki, X. Hu, Energy Environ. Sci. 4 (2011) 3878–3888.
[11] J. Greeley, T.F. Jaramillo, J. Bonde, I.B. Chorkendorff, J.K. Norskov, Nat. Mater. 5 (2006) 909–913.
[12] Q. Yuan, Z.Y. Zhou, J. Zhuang, X. Wang, Chem. Commun. 46 (2010) 1491–1493.
[13] T.F. Jaramillo, K.P. Jorgensen, J. Bonde, J.H. Nielsen, S. Horch, I. Chorkendorff, Science 317 (2007) 100–102.
[14] H. Tang, K.P. Dou, C.C. Kaun, Q. Kuang, S.H. Yang, J. Mater. Chem. A 2 (2014)

360–364.
[15] W.F. Chen, K. Sasaki, C. Ma, A.I. Frenkel, N. Marinkovic, J.T. Muckerman, Y. M. Zhu, R.R. Adzic, Angew. Chem. Int. Ed. 51 (2012) 6131–6135.
[16] M. Nagai, Y. Goto, O. Uchino, S. Omi, Catal. Today 45 (1998) 335–340.
[17] D.V. Esposito, S.T. Hunt, A.L. Stottlemyer, K.D. Dobson, B.E. McCandless, R. W. Birkmire, J.G.G. Chen, Angew. Chem. Int. Ed. 49 (2010) 9859–9862.
[18] Y. Liu, T.G. Kelly, J.G.G. Chen, W.E. Mustain, ACS Catal. 3 (2013) 1184–1194.
[19] P. Xiao, M.A. Sk, L. Thia, X.M. Ge, R.J. Lim, J.Y. Wang, K.H. Lim, X. Wang, Energy Environ. Sci. 7 (2014) 2624–2629.
[20] E.J. Popczun, J.R. McKone, C.G. Read, A.J. Biacchi, A.M. Wiltrout, N.S. Lewis, R. E. Schaak, J. Am. Chem. Soc. 135 (2013) 9267–9270.
[21] X.L. Zheng, J.B. Xu, K. Yan, H. Wang, Z.L. Wang, S.H. Yang, Chem. Mater. 26 (2014) 2344–2353.
[22] Z.C. Xing, Q. Liu, A.M. Arisi, X.P. Sun, Adv. Mater. 26 (2014) 5702–5707.
[23] K. Xiong, L. Li, L. Zhang, W. Ding, L.S. Peng, Y. Wang, S.G. Chen, S.Y. Tan, Z. D. Wei, J. Mater. Chem. A 3 (2015) 1863–1867.
[24] X.M. Geng, W. Wu, N. Li, W.W. Sun, J. Armstrong, A. Al-hilo, M. Brozak, J.B. Cui, T. Chen, Adv. Funct. Mater. 24 (2014) 6123–6129.
[25] D.S. Kong, H.T. Wang, Z.Y. Lu, Y. Cui, J. Am. Chem. Soc. 136 (2014) 4897–4900.
[26] H.F. Liang, L.S. Li, F. Meng, L.N. Dang, J.Q. Zhuo, A. Forticaux, Z.C. Wang, S. Jin, Chem. Mater. 27 (2015) 5702–5711.
[27] Y. Zheng, Y. Jiao, L.H. Li, T. Xing, Y. Chen, M. Jaroniec, S.Z. Qiao, ACS Nano 8 (2014) 5290–5296.
[28] M. Ledendecker, G. Clavel, M. Antonietti, M. Shalom, Adv. Funct. Mater. 25 (2015) 393–399.
[29] H. Vrubel, X.L. Hu, Angew. Chem. Int. Ed. 124 (2012) 12875–12878.
[30] L.G. Feng, H. Vrubel, M. Bensimon, X.L. Hu, Phys. Chem. Chem. Phys. 16 (2014) 5917–5921.
[31] C. Tang, N.Y. Cheng, Z.H. Pu, W. Xing, X.P. Sun, Angew. Chem. Int. Ed. 54 (2015) 9351–9355.
[32] C.G. Morales-Guio, L. Liardet, M.T. Mayer, S.D. Tilley, M. Gratzel, X.L. Hu, Angew. Chem. Int. Ed. 54 (2015) 664–667.
[33] H.C. Zhang, Y.J. Li, G.X. Zhang, P.B. Wan, T.H. Xu, X.C. Wu, X.M. Sun, Electrochim. Acta 148 (2014) 170–178.
[34] L.L. Feng, G.T. Yu, Y.Y. Wu, G.D. Li, H. Li, Y.H. Sun, T. Asefa, W. Chen, X.X. Zou, J. Am. Chem. Soc. 137 (2015) 14023–14026.
[35] J.Q. Tian, Q. Liu, A.M. Asiri, X.P. Sun, J. Am. Chem. Soc. 136 (2014) 7587–7590.
[36] D.N. Liu, Q. Lu, Y.L. Luo, X.P. Sun, A.M. Asiri, Nanoscale 7 (2015) 15122–15126.
[37] X.J. Fan, H.Q. Zhou, X. Guo, ACS Nano 9 (2015) 5125–5134.
[38] L.M. Lang, Y. Shi, J. Wang, F.B. Wang, X.H. Xia, ACS Appl. Mater. Interfaces 7 (2015) 9098–9102.
[39] J.L. Shi, Z.H. Pu, Q. Liu, A.M. Asiri, J.M. Hu, X.P. Sun, Electrochim. Acta 154 (2015) 345–351.
[40] J. Wang, H.X. Zhong, Z.L. Wang, F.L. Meng, X.B. Zhang, ACS Nano 10 (2016) 2342–2348.
[41] Y. Feng, X.Y. Yu, U. Paik, Chem. Commun. 52 (2016) 1633–1636.
[42] X. Zhang, H.M. Xu, X.X. Li, Y.Y. Li, T.B. Yang, Y.Y. Liang, ACS Catal. 6 (2016) 580–588.
[43] J.M. McEnaney, T.L. Soucy, J.M. Hodges, J.F. Callejas, J.S. Mondschein, R. E. Schaal, J. Mater. Chem. A 4 (2016) 3077–3081.
[44] H.B. Zhang, Z.J. Ma, J.J. Duan, H.M. Liu, G.G. Liu, T. Wang, K. Chang, M. Li, L. Shi, X.G. Meng, K.C. Wu, J.H. Ye, ACS Nano 10 (2016) 684–694.
[45] M.F. Shao, F.Y. Ning, M. Wei, D.G. Evans, X. Duan, Adv. Funct. Mater. 24 (2014) 580–586.
[46] W. Ma, R.Z. Ma, C.X. Wang, J.B. Liang, X.H. Liu, K.C. Zhou, T. Sasaki, ACS Nano 9 (2015) 1977–1984.
[47] D.S. Kong, J.J. Cha, H.T. Wang, H.R. Lee, Y. Cui, Energy Environ. Sci. 6 (2013) 3553–3558.
[48] Y.G. Li, H.L. Wang, L.M. Xie, Y.Y. Liang, G.S. Hong, H.J. Dai, J. Am. Chem. Soc. 133 (2011) 7296–7299.
[49] L. Yu, L. Zhang, H.B. Wu, X.W. Lou, Angew. Chem. Int. Ed. 53 (2014) 3711–3714.
[50] S.K. Lee, M.J. Song, J.H. Kim, T.S. Kan, Y.K. Lim, J.P. Ahn, D.S. Lim, NPG Asia Mater. 6 (2014) e115.
[51] X.H. Xiong, G. Waller, D. Ding, D.C. Chen, B. Rainwater, B. Zhao, Z.X. Wang, M. L. Liu, Nano Energy 16 (2015) 71–80.
[52] J. Xu, P. Gao, T.S. Zhao, Energy Environ. Sci. 5 (2012) 5333–5339.
[53] W. Chen, C. Xia, H.N. Alshareef, ACS Nano 8 (2014) 9531–9541.
[54] Q. Liu, J.T. Jin, J.Y. Zhang, ACS Appl. Mater. Interfaces 5 (2013) 5002–5008.
[55] Z.P. Huang, Z.B. Chen, Z.Z. Chen, C.C. Lv, C. Zhang, ACS Nano 8 (2014) 8121–8129.
[56] N. Krstajic, M. Popovic, B. Grgur, M. Vojnovic, D. Sepa, J. Electroanal. Chem. 512 (2001) 16–26.
[57] B.M. Jovic, V.D. Jovic, U.C. Lacnjevac, L. Gajic-krstajic, N.V. Krstajic, Int. J. Hydrog. Energy 40 (2015) 10480–10490.
[58] F. Safizadeh, E. Ghali, G. Houlachi, Int. J. Hydrog. Energy 40 (2015) 256–274.
[59] C.C.L. McCrory, S. Jung, J.C. Peters, T.F. Jaramillo, J. Am. Chem. Soc. 135 (2013) 16977–16987.
[60] J.Q. Tian, Q. Liu, N.Y. Cheng, A.M. Asiri, X.P. Sun, Angew. Chem. Int. Ed. 53 (2014) 9577–9581.
[61] D. Merik, S. Fierro, H. Vrubel, X. Hu, Chem. Sci. 2 (2011) 1262–1267.
[62] Z.B. Chen, D. Cumminst, B.N. Reineche, E. Clark, M.K. Sunkara, T.F. Jaramillo, J. Am. Chem. Soc. 11 (2011) 4168–4175.
[63] J.R. McKone, B.F. Sadtler, C.A. Werlang, N.S. Lewis, H.B. Gray, ACS Catal. 3 (2013) 166–169.
[64] P. Xiao, W. Chen, X. Wang, Adv. Energy Mater. 5 (2015) 1500985.
[65] T.R. Hellstern, J.D. Benck, J. Kibsgaard, C. Hahn, T.F. Jaramillo, Adv. Energy Mater. 6 (2016) 1501758.
[66] Q.F. Wang, X.F. Wang, B. Liu, G. Yu, X.J. Hou, D. Chen, G.Z. Shen, J. Mater. Chem. A 1 (2013) 2468–2473.
[67] H. Wang, G. Wang, Y. Liang, F. Qian, Y. Song, X. Lu, S. Chen, Y. Tong, Y. Li, Nanoscale 7 (2013) 10283–10290.

Lianbo Ma received his M.S. degree in Applied Chemistry from Jiangsu University, PR China (2015). He is now pursing his Ph.D. degree under the supervision of Prof. Zhong Jin and Jie Liu in School of Chemistry and Chemical Engineering, Nanjing University, P.R. China. His main interest is the design and fabrication nanomaterials for energy storage, electrochemistry, and photoelectric conversion.

Yi Hu received his B.S. degree in Chemistry from Sichuan University in 2014. He is now pursuing his M.S. degree under the supervision of Prof. Zhong Jin in School of Chemistry and Chemical Engineering at Nanjing University. His research interests reside in two-dimensional nanomaterials for electrochemical energy storage and photoelectric conversion.

Renpeng Chen has graduated from the Northeastern University (China) since 2014. Now, he is pursuing his M.S. degree under the guidance of Prof. Zhong Jin in School of Chemistry and Chemical Engineering at Nanjing University. His research interest is focused on the synthesis of alloy materials for lithium-ion batteries.

Guoyin Zhu obtained his M.S. degree from Nanjing University of Posts & Telecommunications in 2014. Currently, he is pursuing his Ph.D. degree under the supervision of Prof. Zhong Jin and Jie Liu at Nanjing University. His research is mainly focused on the synthesis of carbonaceous nanomaterials, and their application for energy conversion and storage devices.

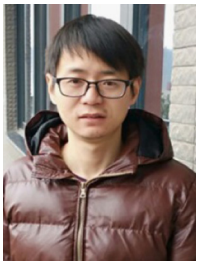

Dr. Tao Chen received his Ph.D. degree in Chemical Engineering and Technology under supervision of Prof. Jiajun Fu from Nanjing University of Science and Technology in June 2015. He is currently a postdoctoral researcher in the group of Prof. Zhong Jin at Nanjing University. His current research focuses on the design and synthesis of nanostructured electrode materials for sodium and lithium ion batteries.

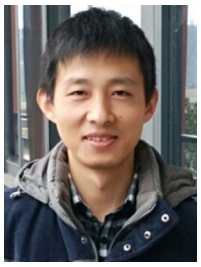

Dr. Hongling Lv received his Ph.D. degree in Materials Processing Engineering under supervision of Professor Jieming Cao from Nanjing University of Aeronautics and Astronautics (2014). He is currently a postdoctoral researcher in the group of Prof. Zhong Jin at Nanjing University. His current research activities focus on key materials for lithium–ion batteries, lithium–sulfur batteries and lithium–selenium batteries.

Yanrong Wang received her master degree in physical chemistry under the supervision of Professor Yong Hu in College of Chemistry and life sciences at Zhejiang Normal University in 2015. She is now pursuing her Ph. D. degree under the supervision of Prof. Zhong Jin and Jie Liu in School of Chemistry and Chemical Engineering at Nanjing University. Her current research interest is the design of new type of battery.

Dr. Jia Liang received his Ph.D. in the Key Laboratory for Physics and Chemistry of Nanodevices from Peking University in 2015, under the guidance of Prof. Gengmin Zhang. He joined Prof. Jun Lou's research group in Rice University as a visiting student in 2014. He is currently an assistant researcher in the group directed by Prof. Zhong Jin and Jie Liu at Nanjing University. His main research interest is synthesis of energy nanomaterials and their applications in solar cells, catalyses, and flow batteries.

Dr. Haixia Liu received her Ph.D. degree from Xiamen University (2014), Xiamen, China. She is currently an assistant researcher in the group directed by Prof. Zhong Jin and Jie Liu at Nanjing University. Her main research interest is the synthesis of nanomaterials and their applications in photoelectrochemistry.

Dr. Changzeng Yan received his Ph.D. degree from Sungkyunkwan University in Korea in August of 2014 under the supervision of Prof. Dae Joon Kang. He is currently working as a postdoctoral research fellow in Prof. Zhong Jin's research group at School of Chemistry and Chemical Engineering, Nanjing University. His research interests include designing and fabrication of novel photocatalysts for solar energy conversion applications: water splitting, CO_2 reduction, and N_2 fixation. He aims to employ varieties of synergistic effects resulting from nano-heterostructures to enhance the energy conversion efficiency.

Dr. Hongfei Zhu received his B.S. (2001) from Huaihai Institute of Technology and Ph.D. (2011) in the Institute of chemistry, CAS. He worked as a postdoctoral scholar at Suzhou Institute of nano-tech and nano-bionics, CAS. Now he is an associate research fellow in School of Chemistry and Chemical Engineering at Nanjing University. His research interest includes: flexible electronics, 2D materials, nanomaterials based electronic devices (include photovoltaic devices, FET, photodetectors, OLEDs, *etc.*).

Dr. Zuoxiu Tie received her B.S. (2004) degree and Ph. D. (2010) from Nanjing University. She is currently a research assistant in the group of Prof. Zhong Jin. Her current research interest focuses on carbonaceous nanomaterials for energy conversion and storage devices.

Prof. Zhong Jin received his B.S. (2003) and Ph.D. (2008) in chemistry from Peking University. He worked as a postdoctoral scholar at Rice University and Massachusetts Institute of Technology. Now he is a professor in School of Chemistry and Chemical Engineering at Nanjing University. He leads a research group working on functional nanomaterials and devices for energy conversion and storage.

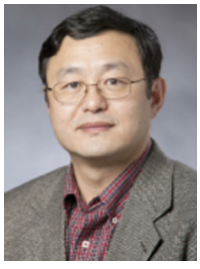

Prof. Jie Liu is currently the George B. Geller Professor of Chemistry at Duke University and an adjunct professor of "Thousands Talents" Program at Nanjing University. He earned a B.S. from Shandong University in 1987 and a Ph.D. from Harvard University in 1996. His research interests include the synthesis and chemical functionalization of nanomaterials, nanoelectronic devices, scanning probe microscopy, and carbon nanomaterials. Prof. Liu is a Fellow of the AAAS, APS and RSC.